Multiscale Finite Element Modeling of the Coupled Nonlinear Dynamics of Magnetostrictive Composite Thin Film

Debiprosad Roy Mahapatra, Debi Prasad Ghosh, and Gopalakrishnan Srinivasan

ARDB Center for Composite Structures, Department of Aerospace Engineering, Indian Institute of Science, Bangalore 560012, India

Abstract. A multiscale nonlinear finite element model for analysis and design of the deformation gradient and the magnetic field distribution in Terfenol-D/epoxy thin film device under Transverse Magnetic (TM) mode of operation is developed in this work. A phenomenological constitutive model based on the density of domain switching (DDS) of an ellipsoidal inclusion in unit cell of matrix is implemented. A sub-grid scale homogenization technique is employed to upwind the microstructural information. A general procedure to ensure the solution convergence toward an approximate inertial manifold is reported.

1 Introduction

In recent time, multiscale modeling and computation have become powerful tool in solving many problems related to strongly coupled dynamics and multiphysics phenomena in material science and engineering [1, 2]. Such an attempt, with judicious choice of the mathematical models which represent the mutually inseparable physical processes at the molecular scale, the lattice scale, the microstructural scale, and at the continuum scale, can be highly reliable in interpreting the experimental results and also in designing new materials and devices with desired multifunctionality. Many similar problems related to fluidics, transport process, biology and planetary sciences are of immense interest in the research community, which requires the advancement of multiscale computational methodology.

The magnetostrictive materials (a family of rare earth compounds), due to large twinning of their magnetic domains, are ideal candidates for high powered microactuators, tunable microwave devices, shape memory devices and bio-inspired systems. Among the majority of magnetostrictive materials, Tb-Dy-Fe type compounds (industrially known as Terfenol-D) are common and show much reduced macroscopic anisotropy [3]. Promising engineering applications are possible using deposited nanostructured film [4, 5], multi-layers [3] and particulate composite [6]. In magnetostrictive polymer thin film, the magnetic domains are essentially constrained and hence behave differently than their bulk samples. Improving the magnetostrictive performance (e.g. larger magnetostriction, smaller hysteresis, wider range of linearity etc.) by sensitizing the dynamic twinning of

V.S. Sunderam et al. (Eds.): ICCS 2005, LNCS 3516, pp. 1–8, 2005.

these magnetic domains under external field is a complex design task which is far from being straightforward using experiments alone and requires detail physical model and intensive computation. Because of the coupled and nonlinear nature of the dynamics, several computational difficulties exist which require special attention.

Ever since the rationale behind the variationally consistent multiscale finite element method was brought out by Hughes *et al.* [7], a tremendous amount of research has been channelized in that path. Among several approaches to tackle the evolvingly complex multiphysics computational mechanics problems, very few approaches, namely the homogenization method [8, 9], the multi-level hierarchical finite element method [10], the level-set method [11] and few others appear promising. In context of time-dependent problems, the concept of consistent temporal integration [12] is worth noting, which extend itself beyond the classical notion of upwinding. Subsequently, while attempting a strongly nonlinear and coupled problem, the advantage in adopting a low-dimensional manifold based on appropriate error estimate during iteration [2, 13] may be noted. In the present paper we report a new variationally consistent multiscale finite model with the following two features: (1) a sub-grid scale for upwinding the miscrostructural information and (2) an approximate manifold of the original system that retains the desired accuracy in the finite element solution, which is unlike the usual ordering scheme as followed in the conventional asymptotic method of truncation.

Our present problem can be described as the magnetostriction induced transformation process in solid state called magnetic domain switching, which occurs in the microscopic scale. In the macroscopic scale, the dynamics is governed through the coupling between elasticity and electromagnetics. The complexity in mathematical modeling is four-fold: (1) describing an accurate constitutive model using phenomenological framework. Here we use a model based on the density of domain switching (DDS) [14], where the series expansion of the Gibbs free energy functional for cubic non-polar crystalline Laves phase is used along with peak piezomagnetic coefficient on the compressive part of the stress acting along the resultant magnetic field vector (2) including the effect of the volume fraction of the magnetostrictive phase in the dilute composite and microstructural pattern (3) retaining only the essential properties of the small scales and nonlinearity and (4) constructing a variationally consistent finite element model and solving it iteratively.

2 Constitutive Model Based on Density of Domain Switching (DDS)

We consider an unit cell of the two phase composite as shown in Fig. 1, in which the ellipsoidal inclusion (B) in matrix phase (A) is the aggregate of magnetostrictive domains. The effective orientation of the magnetic field in these domains is assumed to be at an angle θ which is also the major axis of the ellipsoid. We

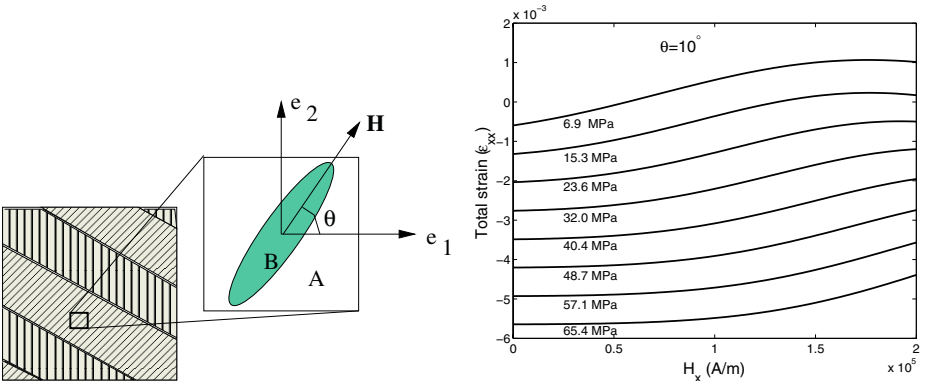

(a) (b)

Fig. 1. (a) Unit cell with oriented magnetostrictive phase B in epoxy matrix phase A (b) strain vs. applied magnetic field in the unit cell with $\epsilon = 0.5$, $\theta = 10^o$ under varying stress

consider an effectively one-dimensional constitutive model of A along the major axis of the ellipsoid. Also, this major axis is assumed to be aligned with the resultant magnetic field $\boldsymbol{H}$ under equilibrium. Using the DDS model [14] it is possible to capture the effect of large magnetostriction more effectively than the other models. According to the DDS model, the piezomagnetic coefficient for the phase B can be written as

$$d = \left[\frac{\partial \varepsilon}{\partial H}\right]_{\sigma} = \tilde{d} e^{-(z-1)^2/A} , \tag{1}$$

where the peak piezomagnetic coefficient $\tilde{d} = \tilde{d}_{cr} + a\Delta\sigma + b(\Delta\sigma)^2$, overstress $\Delta\sigma = \sigma - \sigma_{cr}$, $z = |H|/\tilde{H}$, $\tilde{H} = \tilde{H}_{cr} + \zeta\Delta\sigma$, $A = \sigma_{cr}/\sigma$, σ is the stress, ε is the strain and σ_{cr} is the critical inherent stress of domain switching. a, b, $\tilde{d}_{cr}$, $\tilde{H}_{cr}$ and ζ are material constants obtained by relating the Gibbs free energy and fitting experimental data as discussed in [14]. Let $\epsilon \in (0, 1]$ be the volume fraction of phase B. Applying the mixture rule of rank-one laminate structure under the applied stress components $\{\sigma_{11}, \sigma_{22}, \sigma_{12}\}$ and magnetic field components $\{H_1, H_2\}$ in the unit cell, the constitutive model is obtained, which is expressed in the quasi-linearized form

$$\sigma = \bar{Q}_{AB}\varepsilon - \bar{e}_B H , \quad B = \bar{\mu}_{AB} H + \bar{e}'_B \varepsilon , \tag{2}$$

where ε is the longitudinal strain along the axis of the ellipsoid, B is the magnetic flux density in the film plane, $\bar{Q}_{AB}$ is the effective tangent stiffness, $\bar{e}_B$ and $\bar{e}'_B$ are the tangen coefficients of magnetostriction and $\bar{\mu}_{AB}$ is the effective permeability.

We adopt a quasi-linearization process during time stepping to track the evolution of the morphology in the composite film. Here we first write the coefficients in the constitutive model in Eq. (2) at time $t = t_i$ in terms of the state obtained from the previous time step at $t = t_{i-1} = t_i - \Delta t$ as $\bar{e}^i_B = \bar{e}_B(\epsilon, \sigma^{i-1}, H^{i-1})$,

$\mu^i_{AB} = \mu_{AB}(\epsilon, \sigma^{i-1}, H^{i-1})$. In the subsequent formulation we use the notations: $\boldsymbol{A}.\boldsymbol{B} = A_{ij}B_{jk}$, $\boldsymbol{A} : \boldsymbol{B} = A_{ij}B_{ji}$ as the contraction of tensors over one and two indices, respectively. $|\boldsymbol{A}| := (\boldsymbol{A} : \boldsymbol{A})^{1/2}$. We then rewrite the constitutive model in the coordinate system of the cell (e_1, e_2) as function of the effective angle of orientation $\theta = \theta^i$ of the ellipsoid as

$$\boldsymbol{\sigma} = \boldsymbol{\Gamma}_\varepsilon : \bar{\boldsymbol{Q}}_{AB} : \boldsymbol{\Gamma}_\varepsilon : \boldsymbol{\varepsilon} - \boldsymbol{\Gamma}_\varepsilon : \bar{\boldsymbol{e}}^i_B : \boldsymbol{\Gamma}_H.\boldsymbol{H} =: \bar{\boldsymbol{Q}}^i : \boldsymbol{\varepsilon} - \bar{\boldsymbol{e}}^i.\boldsymbol{H} \ , \tag{3}$$

$$\boldsymbol{B} = \boldsymbol{\Gamma}_H : \bar{\boldsymbol{\mu}}_{AB} : \boldsymbol{\Gamma}_H + \boldsymbol{\Gamma}_H : \bar{\boldsymbol{Q}}^{-1}_B : \boldsymbol{\Gamma}_\varepsilon : \boldsymbol{\sigma} =: \bar{\boldsymbol{e}}^{i^T} : \boldsymbol{\varepsilon} + \bar{\boldsymbol{\mu}}^i.\boldsymbol{H} \ , \tag{4}$$

where $\boldsymbol{\Gamma}_\varepsilon$ is the transformation tensor for strain and stress, $\boldsymbol{\Gamma}_H$ is the transformation tensor for magnetic field vector. Because of the domain switching, the Euler angle θ^i varies over time, which we intend to compute as $\theta^i = \tan^{-1}\left(H^{i-1}_y / H^{i-1}_x\right)$ where $(x, y) \parallel (e_1, e_2)$ and (x, y, z) is the global coordinate system of the composite film.

The electrical source behind the magnetostrictive effect is assumed to be due to the transverse magnetic (TM_z) mode of excitation through array of electrodes parallel to the film plane. We exclude the effect of TE and TEM modes of electromagnetic excitation resulting from any anisotropy in the composite film. Hence $\boldsymbol{H} = \{H_x(x, y, t)\ H_y(x, y, t)\ 0\}^T$ with pointwise prescribed electrical loading $(E_z(z, y, t))$. These should satisfy one of the Maxwell equation for magnetoelectric surface $\nabla \times \boldsymbol{E} = -\dot{\boldsymbol{B}}$, i.e.,

$$\frac{\partial E_z}{\partial x} = -\dot{B}_y \ , \quad \frac{\partial E_z}{\partial y} = \dot{B}_x \ . \tag{5}$$

The deformation can be described by the in-plane displacement and strain

$$\boldsymbol{u} = \{u(x, y, t)\ , v(x, y, t)\ , 0\}^T \ , \quad \boldsymbol{\varepsilon} = \frac{1}{2}(u_{i,j} + u_{j,i}) \ . \tag{6}$$

3 Multiscale Model and Approximate Inertial Manifold

It is important to note that the magnetostriction due to domain switching and the resulting nonlinearity vanishes as $\epsilon \to 0$. In such case, the quasi-linearization of the constitutive law in Eq. (3) results in a linear system whose eigen values are close to that of the slow manifold and a global attractor can be established. Therefore, for $\epsilon \to 0$, it is straightforward to obtain a fairly accurate solution based on center manifold reduction by asymptotic expansion and truncation according to the order of the terms in the PDEs. But in the present case, our objective is to study the film dynamics due to large variation in ϵ spatially or for individual designs with different constituents and manufacturing processes. Therefore, by following the known facts from the reported literature (see [15] and the references therein), we focus our attention on constructing an approximate inertial manifold with global convergence properties in a two-scale finite element framework.

We introduce a slow scale (L_0) and a fast scale (L_1) with the dependent variables defined in them respectively as $(.)_0$ and $(.)_1$, such that

$$\boldsymbol{x}_1 = \boldsymbol{x}/\epsilon \ , \quad t_1 = t/\epsilon \ , \quad \boldsymbol{u} = \boldsymbol{u}_0 + \epsilon \boldsymbol{u}_1 \ , \quad \boldsymbol{H} = \boldsymbol{H}_0 + \epsilon \boldsymbol{H}_1 \tag{7}$$

The dynamics of the thin film can now be described using the momentum conservation law

$$\left(\nabla_0 + \frac{1}{\epsilon}\nabla_1\right).\boldsymbol{\sigma} = \bar{\rho}\frac{\partial^2 \boldsymbol{u}_0}{\partial t^2} + \frac{1}{\epsilon}\bar{\rho}\frac{\partial^2 \boldsymbol{u}_1}{\partial t_1^2} \ , \tag{8}$$

and the source free Maxwell's equation

$$\left(\nabla_0 + \frac{1}{\epsilon}\nabla_1\right).\boldsymbol{B} = 0 \ . \tag{9}$$

In order to introduce the effect of texture of the composite, we perform homogenization. Simplifying Eq. (8) with the help of Eqs. (3) and (5) and homogenizing over a sub-grid S with nodes $j = 1, \cdots, n$, and a prescribed texture

$$\theta^i(x_s, y_s) = \sum_{j=1}^{n} \psi_{\theta j}(x_s, y_s)\theta_j^i \ , \quad \epsilon = \sum_{j=1}^{n} \psi_{\epsilon j}(x_s, y_s)\epsilon_j^i \ , \tag{10}$$

we get

$$\begin{aligned}
&\frac{1}{\Omega_S}\int_{\Omega_S}\Bigg[\bar{\boldsymbol{Q}}^i : \nabla_0.\boldsymbol{\varepsilon} - \nabla_0.\bar{\boldsymbol{e}}^i.\boldsymbol{H} - \bar{\boldsymbol{e}}^i : \nabla_0.\boldsymbol{H} + \frac{1}{\epsilon}\nabla_1.\bar{\boldsymbol{Q}}^i : \boldsymbol{\varepsilon} + \frac{1}{\epsilon}\bar{\boldsymbol{Q}}^i : \nabla_1.\boldsymbol{\varepsilon} \\
&-\frac{1}{\epsilon}\nabla_1.\bar{\boldsymbol{e}}^i.\boldsymbol{H} - \frac{1}{\epsilon}\bar{\boldsymbol{e}}^i : \nabla_1.\boldsymbol{H}\Bigg] d\Omega_S = \frac{1}{\Omega_S}\int_{\Omega_S}\left[\bar{\rho}\frac{\partial^2 \boldsymbol{u}_0}{\partial t^2} + \frac{1}{\epsilon}\bar{\rho}\frac{\partial^2 \boldsymbol{u}_1}{\partial t_1^2}\right] d\Omega_S
\end{aligned} \tag{11}$$

Similarly, homogenization of Eq. (9) gives

$$\begin{aligned}
&\frac{1}{\Omega_S}\int_{\Omega_S}\Bigg[\nabla_0.\bar{\boldsymbol{e}}^{iT} : \boldsymbol{\varepsilon}_0 + \bar{\boldsymbol{e}}^{iT} : \nabla_0.\boldsymbol{\varepsilon}_0 + \frac{1}{\epsilon}\nabla_1.\bar{\boldsymbol{e}}^{iT} : \boldsymbol{\varepsilon}_0 + \nabla_1.\bar{\boldsymbol{e}}^{iT} : \boldsymbol{\varepsilon}_1 + \frac{1}{\epsilon}\bar{\boldsymbol{e}}^{iT} : \nabla_1.\boldsymbol{\varepsilon}_1 \\
&+\nabla_0.\bar{\boldsymbol{\mu}}^i : \boldsymbol{H}_0 + \bar{\boldsymbol{\mu}}^i : \nabla_0.\boldsymbol{H}_0 + \frac{1}{\epsilon}\nabla_1.\bar{\boldsymbol{\mu}}^i : \boldsymbol{H}_0 + \nabla_1.\bar{\boldsymbol{\mu}}^i : \boldsymbol{H}_1 + \frac{1}{\epsilon}\bar{\boldsymbol{\mu}}^i : \nabla_1.\boldsymbol{H}_1\Bigg] d\Omega_S \\
&= 0
\end{aligned} \tag{12}$$

The property of the texture in Eq. (9) is given in terms of the known distribution function ψ_θ and ψ_ϵ. While evaluating Eqs. (11)-(12) we need projection of the nodal variables on the sub-grid nodes. This is done by a least-square fit over the finite element nodal variables $\boldsymbol{u}^{e(i-1)}$, $\boldsymbol{H}^{e(i-1)}$ at time $t = t_{i-1}$ for the elements overlapping with S and by writing

$$\boldsymbol{u}_k = \sum_{j=1}^{n} \psi_{uj}(x_k, y_k, t_{i-1})\boldsymbol{u}_j^e \ , \quad \boldsymbol{\varepsilon}_k = \sum_{j=1}^{n} \psi_{\varepsilon j}(x_k, y_k)\boldsymbol{\varepsilon}_j^e \ ,$$

$$\boldsymbol{H}_k = \sum_{j=1}^{n} \psi_{Hj}(x_k, y_k, t_{i-1})\boldsymbol{H}_j^e \ , \tag{13}$$

where k is an integration point, superscript e indicates finite element nodal quantities. ψ_{uj}^e, $\psi_{\varepsilon j}^e$ and ψ_{Hj}^e are the functions obtained from the least square fit based on the nodal quantities at previous converged time step $t = t_{i-1}$.

3.1 Finite Element Formulation

So far we have just assumed that the values of the finite element nodal variables $\boldsymbol{q}^e = \{\boldsymbol{u}^{eT}\ \boldsymbol{H}^{eT}\}^T$ from the previous time step $t = t_{i-1}$ are known. In order to solve for the variables at $t = t_i$ the finite element equilibrium is now required. First we rewrite Eqs. (11)-(12) as respectively

$$\mathcal{L}_1(\partial_t, \partial_{t1})\boldsymbol{g}(\boldsymbol{u}_0, \boldsymbol{u}_1) - \mathcal{L}_2(\nabla_0, \nabla_1)\boldsymbol{p}(\boldsymbol{\varepsilon}_0, \boldsymbol{\varepsilon}_1, \boldsymbol{H}_0, \boldsymbol{H}_1) = 0\ , \tag{14}$$

$$\mathcal{L}_3(\nabla_0, \nabla_1)\boldsymbol{g}(\boldsymbol{\varepsilon}_0, \boldsymbol{\varepsilon}_1, \boldsymbol{H}_0, \boldsymbol{H}_1) = 0\ , \tag{15}$$

The final step to obtain our two-scale finite element model is the variational minimization of the weak form, which can be written in the form

$$\delta \int_\Omega \boldsymbol{u}.\left[\mathcal{L}_1\boldsymbol{g} - \mathcal{L}_2\boldsymbol{p}\right] d\Omega + \delta \int_\Omega \boldsymbol{H}.\mathcal{L}_3\boldsymbol{g} d\Omega = 0\ , \tag{16}$$

which leads to the global finite element equilibrium equation

$$\boldsymbol{M}_0\ddot{\boldsymbol{q}}_0^e + \boldsymbol{M}_1\ddot{\boldsymbol{q}}_1^e + \boldsymbol{K}_0\boldsymbol{q}_0^e + \boldsymbol{K}_1\boldsymbol{q}_1^e = \boldsymbol{f}\ . \tag{17}$$

Eq. (17) is further condensed out by eliminating the magnetic field vector $\boldsymbol{H}^e$ by using the pointwise magnetic excitation condition in Eq. (5) rewritten as

$$\left\{\begin{array}{c} H_x \\ H_y \end{array}\right\} = (\bar{\boldsymbol{\mu}}^i)^{-1} : \left\{\begin{array}{c} \displaystyle\int_{t_{i-1}}^{t_i} \frac{\partial E_z}{\partial y} dt \\ \displaystyle -\int_{t_{i-1}}^{t_i} \frac{\partial E_z}{\partial x} dt \end{array}\right\} - (\bar{\boldsymbol{\mu}}^i)^{-1} : \bar{\boldsymbol{e}}^{iT} : \boldsymbol{\varepsilon}\ . \tag{18}$$

In the present problem when $\epsilon \to 0$, the dynamics is that of semilinear elliptic PDEs in $(\boldsymbol{u}, \boldsymbol{H})$, hence usual bi-linear element with mesh density comparable with the wavenumber of the magnetic excitation is sufficient to produce accurate result. However, such properties no longer hold for $\epsilon \to 1$. Also, $\epsilon\nabla$ is not bounded. A suitable approach in related context of obtaining an approximate manifold (h) is to fix the spatial discretization at a given time step and obtain the approximate solution

$$\boldsymbol{u} = \boldsymbol{u}_0 + \epsilon\boldsymbol{u}_1 = \boldsymbol{u}_0 + \epsilon\boldsymbol{h}(\boldsymbol{u}_0)\ , \tag{19}$$

through iteration. In order to derive the condition to iterate over $\boldsymbol{h}$ while solving Eq. (17), we take help of *apriori* error estimates. Since such an error estimate should ideally be independent of the choice of the scales, i.e. irrespective of the fact that the system is slow (or fast) in that scale [16], we first set $\boldsymbol{u}_0 = \boldsymbol{0}$, $\boldsymbol{H}_0 = \boldsymbol{0}$. Neglecting the inertia terms in the strong form corresponding to Eqs. (11)-(12) and rearranging, we get

$$\nabla_1.\boldsymbol{\varepsilon}_1 = \boldsymbol{R}_1^i : \boldsymbol{\varepsilon} + \boldsymbol{R}_2^i : \boldsymbol{H}_1\ , \quad \nabla_1.\boldsymbol{H}_1 = \boldsymbol{R}_3^i : \boldsymbol{\varepsilon} + \boldsymbol{R}_4^i : \boldsymbol{H}\ , \tag{20}$$

where $\boldsymbol{R}_1^i$, $\boldsymbol{R}_2^i$, $\boldsymbol{R}_3^i$ and $\boldsymbol{R}_4^i$ are functions of $(\epsilon, \theta^i, \boldsymbol{\sigma}^{i-1}, \boldsymbol{H}^{i-1})$ at time $t = t_{i-1}$. We consider a strong estimate

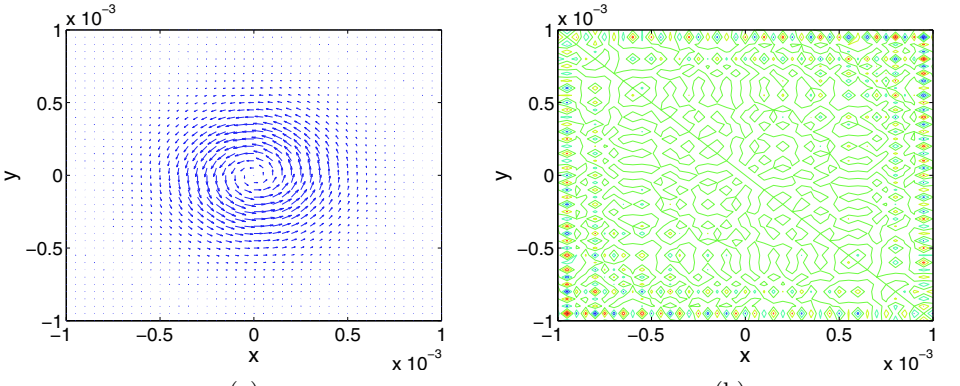

Fig. 2. (a) Orientation of $\boldsymbol{H}$ field vectors and (b) shear strain contour under normally applied short pulse $E_z(t)$ and captured at $t = 50ns$

$$\left(\frac{\partial}{\partial t_1} + \epsilon\nabla_1\right)\left(|\boldsymbol{\varepsilon}_1|^2 + |\boldsymbol{H}_1|^2\right) = 2\boldsymbol{\varepsilon}_1 : \frac{\partial \boldsymbol{\varepsilon}_1}{\partial t_1} + 2\epsilon\boldsymbol{\varepsilon}_1 : \nabla_1.\boldsymbol{\varepsilon}_1$$
$$+2\boldsymbol{H}_1 : \frac{\partial \boldsymbol{H}_1}{\partial t_1} + 2\epsilon\boldsymbol{H}_1 : \nabla_1.\boldsymbol{H}_1 \tag{21}$$

Using Eq. (20) in Eq. (21) and applying the elementary inequality $uv \leq \beta u^2 + v^2/\beta$, finally we get

$$\left(\frac{\partial}{\partial t_1} + \epsilon\nabla_1\right)\left(|\boldsymbol{\varepsilon}_1|^2 + |\boldsymbol{H}_1|^2\right) \leq -2\gamma_1^i|\boldsymbol{\varepsilon}_2|^2 - 2\gamma_2^i|\boldsymbol{H}_1|^2 - 2\gamma_3^i|\dot{\boldsymbol{\varepsilon}}_1|^2 - 2\gamma_4^i|\dot{\boldsymbol{H}}_1|^2\,, \tag{22}$$

where $\dot{(\,)} := \partial/\partial t_1$, γ_1^i, γ_2^i, γ_3^i γ_4^i are functions of $(\epsilon, \theta^i, \boldsymbol{\sigma}^{i-1}, \boldsymbol{H}^{i-1})$. Integrating Eq. (22) along the characteristic line $\partial/\partial t_1 + \epsilon\nabla_1 =$ constant, between the interval (t_{i-1}, t_i), and by taking sup on $(x, y) \in S^1$, we have

$$||\boldsymbol{\varepsilon}_1||^2 + ||\boldsymbol{H}_1||^2 \leq e^{-\gamma_1^i \Delta t}||\boldsymbol{\varepsilon}_1^{i-1}||^2 + e^{-\gamma_2^i \Delta t}||\boldsymbol{H}_1^{i-1}||^2$$
$$+e^{-\gamma_3^i \Delta t}||\dot{\boldsymbol{\varepsilon}}_1^{i-1}||^2 + e^{-\gamma_4^i \Delta t}||\dot{\boldsymbol{H}}_1^{i-1}||^2\,. \tag{23}$$

We use Eq. (23) and Newmark's finite difference scheme in time to solve Eq. (17) concurrently in $(\boldsymbol{q}_0^e, \boldsymbol{q}_1^e)$. Fig. 2 shows the snap of the evolved field patterns simulated in case of $Tb_{0.27}Dy_{0.73}Fe_{1.95}$-epoxy(30% by vol.) film under nanosecond electrical pulse applied at the center.

4 Concluding Remarks

Based on a phenomenological microscopic model of magnetostrictive polymer composite material, and macroscopic dynamics, a multiscale finite element model with subgrid-scale homogenization is formulated. Error estimates are derived. Numerical simulation of the time-resolved field pattern in Terfenol-D polymer is reported.

References

1. Ghoniem, N.M., Busso, P., Kioussis, N. and Huang, H.: Multiscale modelling of nanomechanics and micromechanics: an overview. Phil. Mag. **83**(31-34) (2003) 3475–3528
2. Melnik, R.V.N. and Roberts, A.H.: Computational models for multi-scale coupled dynamic problems. Future Generation Computer Systems **20** (2004) 453–464
3. Quandt, E., Ludwig, A., Mencik, J. and Nold E.: Giant magnetostrictive TbFe/Fe multilayers. J. Alloys Compounds **258** (1997) 133–137
4. Kumar, D., Narayan, J., Nath, T.K., Sharma, A.K., Kvit, A. and Jin, C.: Tunable magnetic properties of metal ceramic composite thin film. Solid State Communications **119** (2001) 63–66
5. Liu, T., Burger, C. and Chu B.: Nanofabrication in polymer matrices. Prog. Polym. Sci. **2003** 5–26
6. Hommema, J. A.: Magnetomechanical behavior of Terfenol-D particulate composites. MS Thesis, University of Illinois at Urbana-Champaign (1999)
7. Hughes, T.J.R., Feijoo, G.R., Mazzei, L., and Quincy, L.B.: The variational multiscale method – a paradigm for computational mechanics. Computer Methods in Applied Mechanics and Engineering **166** (1998) 3–24
8. Babuska, I.: Homogenization approach in engineering, in: Lions, R., Glowinski (Eds.), Computing Methods in Applied Sciences and Engineering, Lecture Notes in Economics and Mathematical Systems **134** (1976) Springer, Berlin
9. Terada, K. and Kikuchi, N.: A class of general algorithms for multiscale analysis of heterogeneous media. Comput. Methods Appl. Nech. Engrg. **190** (2001) 5427–5464
10. Calgero, C., Laminie, J. and Temam, R.: Dynamical multilevel schemes for the solution of evolution equations by hierarchical finite element discretization. Appl. Numer. Math. **23** (1997) 403–442
11. Chessa, J. and Belytschko, T.: Arbitrary discontinuities in space-time finite elements by level sets and X-FEM. Int. J. Numer. Meth. Engng. **61** (2004) 2595–2614
12. Bottasso, C.L.: Multiscale temporal integration. Comput. Methods Appl. Mech. Engrg. **191** (2002) 2815–2830
13. Margolin, L.G., Titi, E.S. and Wynne, S.: The postprocessing Galerkin and nonlinear galerkin methods - A truncation analysis point of view. SIAM J. Numer. Anal. **41** (2003) 695–714
14. Wan, Y., Fang, D., Hwang, K.-C.: Non-linear constitutive relations for magnetostrictive materials. Int. J. Non-linear Mechanics **38** (2003) 1053–1065
15. Steindl, A. and Troger, H.: Methods for dimension reduction and their application in nonlinear dynamics. Int. J. Solids Struct. **38** (2001) 2131–2147
16. Menon, G. and Haller, G.: Infinite dimensional geometric singular perturbation theory for the Maxwell-Bloch equations. SIAM J. Math. Anal. **33** (2001) 315–346